

TRI-PP-93-4
Jan 1993

$\pi \rightarrow e\nu$ Decay; Window on the Generation Puzzle

Douglas A. Bryman
TRIUMF, 4004 Wesbrook Mall, Vancouver, B.C., Canada V6T 2A3

Abstract

Two recent measurements of the $\pi \rightarrow e\nu/\pi \rightarrow \mu\nu$ branching ratio have been made with reported precision of 0.4%. A stringent test of the standard model hypothesis of electron-muon universality follows since the theoretical prediction including radiative corrections is unambiguous at the level of 0.1%. Other aspects of standard and non-standard models such as mixing of massive neutrino eigenstates and Majoran couplings can also be constrained by examination of these results.

(submitted to Comments on Nuclear and Particle Physics)

1. INTRODUCTION

While the standard model (SM) has been extremely successful in describing presently observed phenomena, it has little to say about the existence of or relation between the multiple generations or flavors. One possible hint is found in the necessity of having three quark generations to accommodate CP violation in the Cabibbo-Kobayashi-Maskawa (CKM) mixing matrix although this is far from established experimentally. In the lepton sector, the three charged particles, e , μ and τ and their associated neutrinos are unmixed and their interactions appear to be universal. Extensive attempts to observe lepton flavor changing reactions which would indicate physics beyond the SM have met with only null results so far.

Precise measurements of the decays of leptons and mesons play a significant role in challenging the SM by searching for deviations from its predictions and thereby aiming to uncover effects which would indicate new directions. Purely leptonic weak processes like $\mu \rightarrow e\nu\bar{\nu}$ and $\tau \rightarrow e\nu\bar{\nu}$ decays are particularly amenable to confrontation of experimental measurements with high precision SM calculations including radiative corrections. However, when hadrons are explicitly involved, although the phenomenology is potentially enriched, strong interaction effects generally complicate the attempt to do reliable calculations and extract unambiguous inferences from comparison with experimental results. This is the case in evaluation of the CP violation parameter ratio ϵ'/ϵ obtained in $K \rightarrow \pi\pi$ experiments and in detailed studies of $K_L^0 \rightarrow \mu\mu$ and neutron beta decays where nonperturbative strong interaction physics dominate the hadronic matrix elements.

However, there are a few exceptional weak processes involving hadrons which, due to symmetries or special circumstances, can be calculated to unusually high precision and lead to important tests of the SM because they are also accessible to accurate measurements. One class of processes which fall into this category is superallowed beta decay. Due to the conserved vector current, when $0^+ \rightarrow 0^+$ Fermi transitions (with small $O(\alpha)$ corrections) are compared with muon decay a precise value of the CKM element $V_{ud} = 0.9750 \pm 0.0007$ (Ref.¹) can be extracted.²

The $\pi \rightarrow e\nu/\pi \rightarrow \mu\nu$ branching ratio is a special case involving meson decays which, as a consequence of gauge invariance, can be calculated to a surprisingly low level of theoretical uncertainty, $< 0.1\%$ including radiative corrections. This situation occurs in spite of the presence of pion structure dependent effects which generally spoil attempts to precisely calculate reactions involving light quarks. The $\pi \rightarrow e\nu$ branching ratio allows the best test of the SM hypothesis of lepton universality to be obtained since measurements with 0.4% experimental uncertainties have been reported recently. The experiments take advantage of the ability to measure the ratio of decay processes $\pi \rightarrow e\nu$ and $\pi \rightarrow \mu\nu$ followed by $\mu \rightarrow e\nu\nu$ ($\pi \rightarrow \mu \rightarrow e$ chain) thereby removing many potential systematic uncertainties. In this article, the latest theoretical and experimental results on $\pi \rightarrow e\nu$ decay will be discussed leading to another triumph for the SM, further limitations on its extensions, and a deepening of the lepton generation puzzle.

2. $\pi \rightarrow e\nu$ in the Standard Model

Lepton universality is firmly embedded in the minimal SM. Deviations would have significant consequences for the gauge structure of the theory. For instance, non-

¹In the future, precise measurements of V_{ud} from pion beta decay $\pi^+ \rightarrow \pi^0 e^+ \nu$ may also become available.

universality might imply separate degenerate gauge bosons for each generation or the existence of a lepton mixing matrix in analogy with the CKM matrix if neutrinos are massive. Deviations of experimental measurements from the expectation of universality could also arise due to the presence of new physics such as the existence of additional heavy neutrino generations,² new gauge bosons, substructure, Majorons,³ or charged Higgs scalars arising from extended symmetries.⁴ Neutral current universality is examined in measurements of $Z \rightarrow l^+l^-$ decays where l represents e, μ or τ . Charged current universality is tested most effectively in π, τ and W leptonic decays and a particularly sensitive measure of $e - \mu$ universality has been derived from study of $\pi \rightarrow e\nu$ decay.

Since the pion is a pseudoscalar particle it can be determined on grounds of Lorentz invariance in the context of the SM that the hadronic matrix element for $\pi^+ \rightarrow l^+\nu$ decay has only an axial vector component

$$\langle 0 | A_\lambda(0) | \pi \rangle = i f_\pi(q^2) q_\lambda \quad (1)$$

where q is the four-momentum of the pion and $f_\pi(q^2) = f_\pi(-m_\pi^2) \equiv f_\pi$ is the pion decay constant. Early calculations of the $\pi \rightarrow e\nu$ branching ratio including radiative effects were done by Berman⁶ and Kinoshita⁷ and resulted in a value

$$R_{\pi e\nu} = \frac{\Gamma(\pi \rightarrow e\nu + \pi \rightarrow e\nu\gamma)}{\Gamma(\pi \rightarrow \mu\nu + \pi \rightarrow \mu\nu\gamma)} = R_0 \left(1 + 3 \frac{\alpha}{\pi} \ln \frac{m_e}{m_\mu} \right) \left(1 - 0.92 \frac{\alpha}{\pi} \right) = 1.233 \times 10^{-4}. \quad (2)$$

$R_0 = \frac{m_e^2 (m_\pi^2 - m_e^2)^2}{m_\mu^2 (m_\pi^2 - m_\mu^2)^2} = 1.28 \times 10^{-4}$ is the branching ratio without radiative effects included. The radiative corrections in Eq. 2 depended on an ultra-violet cutoff assumed equal for electrons and muons. Similar results were subsequently obtained by Goldman and Wilson⁸ who employed a series of modern gauge theory model approaches. These calculations were followed by definitive theoretical work of Marciano and Sirlin⁹ who proved that, in the SM, the largest contribution to the radiative correction in the $\pi \rightarrow e\nu$ branching ratio, $3(\alpha/\pi)h(m_e/m_\mu)$, is a direct consequence of gauge invariance. Consider an expansion of the decay rate $\Gamma = \Gamma(\pi \rightarrow l\nu + \pi \rightarrow l\nu\gamma)$ in a series involving $\ln m_l$ and m_l^2 :

$$\Gamma_l = \Gamma_l^0 \left[1 + \frac{\alpha}{\pi} (C_0 \ln m_l + C_1 + C_2 m_l^2 \ln m_l + C_3 m_l^2 + \dots) \right] \quad (3)$$

where Γ_l^0 is the $\pi \rightarrow l\nu$ decay rate without radiative corrections. The coefficient of the logarithmic lepton mass singularity (l.m.s.) term C_0 is not modified by the strong interactions. The value $C_0 = 3$ was given correctly by the calculation of Kinoshita. The term C_1 is independent of m_l and therefore cancels in the branching ratio. C_2 and C_3 lead to small contributions since by dimensionality $C_{2,3} \sim 1/M^2$ where M is some typical hadronic mass, for example, m_p or m_π .

Aside from the diagrams of Figs. 1a and 1b calculated by Kinoshita, who accounted for all $\mathcal{O}(\alpha)$ m_π dependence, the only virtual photon diagram that contributes to the l.m.s. is shown in Fig. 1c. Using gauge invariance, Marciano and Sirlin found that the inner bremsstrahlung contributions from the diagrams in Fig. 1c resulted in terms identical to those calculated by Kinoshita plus an additional term due to interference between the strong interaction-independent amplitude and the structure-dependent part of the amplitude. This interference term resulted in a correction

which exactly canceled the structure-dependent contribution from the virtual corrections. Thus, all contributions to the l.m.s. vanished except the term $3(\alpha/\pi) \ln m_l$ which is a consequence of gauge invariance. The contribution of the remaining l.m.s. to the branching ratio $R_{\pi e\nu}$ is a correction of -3.7%. Structure dependent effects which could be important in the $\pi \rightarrow e\nu\gamma$ decay are estimated to be at the level of < 0.1%. For the cases of heavier pseudoscalar meson decays such as $K \rightarrow l\nu\gamma$ and $D \rightarrow l\nu\gamma$ the structure-dependent terms are expected to be much larger.

The calculated value¹⁰ of the $\pi \rightarrow e\nu$ branching ratio is

$$R_{\pi e\nu}^{\text{th}} = (1.234 \pm 0.001) \times 10^{-4} \quad (4)$$

where the estimated theoretical uncertainty arises from uncalculated but bounded pion structure effects which are suppressed by $\alpha/\pi \ln^2 \ln \frac{m_e}{m_\pi}$. Prior to the recent work discussed below, the experimental result,¹¹ $R_{\pi e\nu} = (1.218 \pm 0.014) \times 10^{-4}$, was sufficient to confirm the theory at the 1% level.

3. $\pi \rightarrow e\nu$ Experiments

3.1. TRIUMF experiment

In the recent measurement of the $\pi \rightarrow e\nu$ branching ratio performed at TRIUMF,¹² the strategy used for reducing systematic uncertainties was to make measurements of the positrons from both $\pi \rightarrow e\nu$ and the $\pi - \mu - e$ decay chain with a non-magnetic electromagnetic detector. In this technique, employed earlier by DiCapua *et al.*¹³ and later by Bryman *et al.*,¹¹ the efficiencies and acceptances were the same for the numerator and denominator of the branching ratio over the full range of positron energies except for small energy dependent effects (such as multiple Coulomb scattering). The measurement then required the determination of the ratio of the number of positrons in the $\pi \rightarrow e\nu$ peak to those from the $\pi \rightarrow \mu \rightarrow e$ chain, applying small timing and geometrical corrections. The largest correction to the basic measurement, $\mathcal{O}(1\%)$, and the main potential source of systematic uncertainty came from the characteristic low-energy tail of the finite size electromagnetic calorimeter which resulted in some small part (including a radiative decay contribution) of the $\pi \rightarrow e\nu$ peak extending under the 10^4 times more intense $\pi \rightarrow \mu \rightarrow e$ distribution.

The setup for the TRIUMF measurement is shown in Fig. 2. Decay positrons from stopped pions were detected at 90° to the beam passing through two planar wire chambers (WC) for position measurement, and scintillators T1 - T4, before being stopped and energy-analyzed in a 460-mm diam. \times 510-mm long NaI(Tl) crystal "FINA". The positron energy spectrum consisted of a peak at 69 MeV from $\pi \rightarrow e\nu$ decay and a distribution from 0 to 53 MeV from the $\pi \rightarrow \mu \rightarrow e$ chain as shown in Fig. 3a.

In order to measure the low energy tail component of the response function that contributed to the $\pi \rightarrow e\nu$ events, it was necessary to suppress the dominant $\pi \rightarrow \mu \rightarrow e$ component. This was done by applying two techniques. First, exploiting the short pion lifetime (26 ns) compared to the muon lifetime (2 μ s), positrons accepted only in the first 30 ns after the pion stops were enriched in $\pi \rightarrow e\nu$ events by a factor of 100. The resulting energy spectrum is shown in Fig. 3a. The second technique utilized the absence of the extra 4.2 MeV deposited in the pion stop counter (B3) from $\pi - \mu$ decay to select direct $\pi - e$ events. This resulted in an additional suppression of $\pi \rightarrow \mu \rightarrow e$ events by a factor of 1000 as shown in Fig. 3b. The $\pi \rightarrow e\nu$ spectrum

with the background suppressed was then analyzed to determine that $1.93 \pm 0.25\%$ of $\pi \rightarrow e\nu$ events underlie the $\pi \rightarrow \mu \rightarrow e$ distribution which extended from 53 MeV down to zero.

The branching ratio was determined by simultaneous fitting of the time spectra shown in Fig. 4 for events above and below the energy threshold 53 MeV corresponding primarily to $\pi \rightarrow e\nu$ and $\pi \rightarrow \mu \rightarrow e$ events, respectively. Many potential systematic effects were evaluated from the data and simulated using Monte Carlo methods including possible rate-dependences, effects due to energy dependent radiative processes such as positron annihilation-in-flight and multiple Coulomb scattering of positrons and electrons leading to pathological triggers, false vetoes, and lost low-energy positrons. The multiplicative correction to the raw branching ratio from Monte Carlo calculations was 1.0027 ± 0.0011 and other small corrections were obtained from the data as indicated in Table I. The final result was $R_{\pi e\nu}^{\text{exp}} = 1.2265 \pm 0.0034(\text{stat}) \pm 0.0044(\text{sys}) \times 10^{-4}$, in good agreement with the SM expectation $R_{\pi e\nu}^{\text{th}}$.

3.2. PSI experiment

An experiment¹⁴ performed at PSI used a similar technique to obtain results with comparable precision. This effort employed a 4π sr BGO spectrometer shown in Fig. 5 to measure the total energy of the incident pion and its decay products. The branching ratio was determined by obtaining the number of $\pi \rightarrow e\nu(\gamma)$ decays divided by the number of $\pi \rightarrow \mu\nu(\gamma)$ decays observed in a time interval from 7.5 to 200 ns following the pion stop in the target counter, T. The T counter was instrumented with a high speed digitizer to identify the $\pi \rightarrow e\nu$ decay as a sequence of two pulses from the stopping pion and the positron accompanied by an electromagnetic shower in the 18 radiation lengths thick calorimeter. $\pi - \mu - e$ decay chain events gave three pulses in the target with an identifiable 4.2 MeV muon pulse. In this technique, which compares positrons from $\pi \rightarrow e\nu$ decay with muons from $\pi \rightarrow \mu\nu$ decay, radiative muon decay (RMD) complicated the identification of $\pi \rightarrow e\nu$ events when only the total energy of the event was used because in RMD the sum of the positron and photon energies measured in the 4π geometry extends up to the muon rest mass $m_\mu = 105.6$ MeV. As in the TRIUMF experiment the low energy tail of the spectrometer's resolution function must also be accounted for to determine the number of $\pi \rightarrow e\nu$ events in the low energy region.

The 132 element spectrometer gave energy resolution of 4% FWHM at 90 MeV and timing resolution for showers good to ± 1 ns. The plastic scintillator T counter, read out through BGO crystals, obtained a resolution of $\pm 2.5\%$ at 20 MeV for the beam pions. Data from the T counter was subjected to stringent off-line cuts to reduce backgrounds associated with the pion stop signals. Fig. 6 shows the total energy spectrum after cuts were applied, divided into three regions; the central window contained most $\pi \rightarrow e\nu\gamma$ events and the two regions below and above were dominated by backgrounds from $\pi - \mu - e$ chain events and pion interactions in the target. To correct the number of $\pi \rightarrow e\nu\gamma$ events in the central region for low energy losses, the electromagnetic shower in the spectrometer was simulated using Monte Carlo methods including effects due to photonuclear processes. As indicated in Table II, the corrections for electromagnetic and photonuclear losses were estimated to be $1.64 \pm 0.09\%$ and $0.95 \pm 0.2\%$, respectively. The other large correction, due to RMD, was determined from the data. The final result reported recently was $R_{\pi e\nu}^{\text{exp}} = 1.235 \pm 0.005 \times 10^{-4}$ in good agreement with the value from the TRIUMF experiments.

Combining the PSI¹⁴ and TRIUMF^{11,12} results gives

$$R_{\pi e\nu}^{\text{exp}} = 1.2303 \pm 0.0036 \times 10^{-4} \quad (5)$$

4. Interpretation

A quantitative test of the hypothesis of $e - \mu$ universality can be obtained by writing

$$R_{\pi e\nu}^{\text{exp}} = \left(\frac{g_e}{g_\mu}\right)^2 R_{\pi e\nu}^{\text{th}} \quad (6)$$

where g_e and g_μ are the relative electroweak couplings of e and μ . The result from Eqs. (4) and (5) is

$$g_e/g_\mu = 0.9985 \pm 0.0015 \quad (7)$$

in agreement with the hypothesis of $e - \mu$ universality where a value of unity would correspond to perfect universality. Other measures of $e - \mu$ (as well as $\tau - e$ and $\tau - \mu$) universality have been obtained from ν_e and ν_μ charged current interactions, and from τ and W leptonic decays. While less accurate than the other tests, the $W \rightarrow l\nu$ measurements are valuable since they confirm universality at higher mass scales and don't rely on π or τ branching ratios.

$\tau - e$ universality can also be examined by comparison¹⁵ of the $\pi \rightarrow e\nu$ and $\tau \rightarrow \pi\nu$ decay rates using the π and τ lifetimes:

$$\frac{\Gamma(\tau \rightarrow \pi\nu)}{\Gamma(\pi \rightarrow e\nu)} = \left(\frac{g_\tau}{g_e}\right)^2 \frac{R_\mu^{\text{th}}}{R_{\pi e\nu}^{\text{th}}} \quad (8)$$

where R_μ^{th} is the ratio of rates for $\tau \rightarrow \pi\nu$, and $\pi \rightarrow \mu\nu$ decays.¹⁶ Using the latest values for the branching ratio $B_\pi = \frac{\Gamma(\tau \rightarrow \pi\nu)}{\Gamma(\tau \rightarrow \text{all})} = 0.116 \pm 0.004$ ¹⁷ and the recently reported precise value of the τ mass $m_\tau = 1776.9_{-0.5}^{+0.4} \pm 0.2$ MeV¹⁸ one finds

$$\frac{g_\tau}{g_e} = 1.014 \pm 0.027 \quad (9)$$

Direct comparison of τ , with τ_π results in a test of $\tau - \mu$ universality:

$$\frac{g_\tau}{g_\mu} = \left[\frac{\tau_\pi B_\pi}{\tau_\tau R_\mu^{\text{th}}} \right]^{\frac{1}{2}} = 1.012 \pm 0.021 \quad (10)$$

A small discrepancy had been noted¹⁹ in accurate measures of $\tau - e$ and $\tau - \mu$ universality derived from comparison of the τ lifetime (τ_τ) and the μ lifetime (τ_μ) in conjunction with the measured branching ratios¹⁷ for $\tau \rightarrow e\nu e\nu$, and $\tau \rightarrow \mu\nu \mu\nu$ decays, $B_e = 0.1793 \pm 0.0026$ and $B_\mu = 0.1758 \pm 0.0027$. The current result for g_τ/g_μ is

$$\frac{g_\tau}{g_\mu} = \left[\frac{\tau_\mu}{\tau_\tau} \left(\frac{m_\mu}{m_\tau}\right)^5 B_e \right]^{\frac{1}{2}} = 0.980 \pm 0.012 \quad (11)$$

Similarly, using the measured and calculated values for $\tau \rightarrow \mu\nu\nu$, one finds $g_\tau/g_e = 0.984 \pm 0.012$. The nearly two standard deviation discrepancies from universality might be due to statistical fluctuations, or could be the result of unspecified errors in the determination of the (world average values) of τ , m_τ , or B_e and B_μ . However, as a consequence of changes to B_τ and m_τ , if the results using $\tau \rightarrow \pi\nu$ (Eqs. 9 and 10) are averaged with those using $\tau \rightarrow l\nu\nu$ the problem apparently disappears. Tables III, IV and V summarize the latest results on $e - \mu$, $\tau - \mu$ and $\tau - e$ universality.

In addition to testing universality the $\pi \rightarrow e\nu$ results, by virtue of the precise SM prediction, can serve to place constraints on other non-SM approaches. For instance, helicity suppression of $\pi \rightarrow e\nu$ would be absent if the decay was dominated by a pseudoscalar coupling and the $\pi \rightarrow e\nu$ branching ratio would be $\Gamma_0^{e\nu} = (m_\pi^2 - m_e^2)^2 / (m_\pi^2 - m_\mu^2)^2 = 5.5$. An estimate of the contribution of such an interaction can be obtained by subtracting the SM component from the experimental result Eq. 5 and attributing the remainder to a pseudoscalar coupling:

$$f_p = (-0.0015 \pm 0.0015) f_p m_e. \quad (12)$$

Massive charged Higgs particles (m_{H^\pm}) with certain couplings (i.e. those proportional to heavy fermion masses), pseudoscalar leptoquarks ($m_{p\ell}$), vector leptoquarks ($m_{p\nu}$) and supersymmetric particles could all make pseudoscalar contributions which would show up in interference with the SM $\pi \rightarrow e\nu$ amplitude. Some possibilities discussed by Shanker¹¹ are shown in the diagrams of Fig. 7. Interference effects resulting in changes to the $\pi \rightarrow e\nu$ branching ratio would vary as m_h^{-2} where m_h is the mass of the hypothetical heavy particle involved, in contrast to the m_h^{-4} dependence of typical lepton flavor violating interactions. Mass limits for maximal coupling $m_{H^\pm} > 2$ TeV, $m_{p\ell} > 1.3$ TeV and $m_{p\nu} > 220$ TeV can be obtained from the $\pi \rightarrow e\nu$ branching ratio results quoted above.

Other new electroweak effects could be revealed by a discrepancy between $R_{\pi\tau}^{e\nu}$ and the SM prediction. A decay of the form $\pi \rightarrow e\nu M$ where M is a new scalar, pseudoscalar, vector or pseudovector particle with mass ranging from 0 to m_π is of interest.²⁴ For short lifetimes ($\tau_M < 10^{-10}$ s) decays $M \rightarrow e^+e^-$ have been severely constrained.²⁵ One candidate for M is the Majoron, a Nambu-Goldstone boson which appears in models like that proposed by Gelmini and Roncadelli²⁶ where neutrino mass arises from the vacuum expectation value of a weak isotriplet scalar Higgs boson. The calculated ratio for decays involving Majorons or light Higgs bosons χ ($m < 1$ MeV) to the usual processes is

$$r^{Mh} = \frac{\Gamma(\pi \rightarrow eL^0)/\Gamma(\pi \rightarrow eL^0)}{\Gamma(\pi \rightarrow e\nu)/\Gamma(\pi \rightarrow \mu\nu)} = 1 + 157.5 g^2 \quad (13)$$

where L^0 includes the final states $\nu, \nu\chi$ and νM and g^2 is the Majoron-neutrino coupling. Using the theoretical and experimental results, the ratio $r = \frac{R_{\pi\tau}^{e\nu}}{R_{\pi\tau}^{\mu\nu}} < 1.0038$ (90% C.L.) is obtained. Equating Eq. (13) with r results in

$$g^2 < 2.4 \times 10^{-5}. \quad (14)$$

The branching ratios for $\pi \rightarrow e\nu M$, where M is any unobserved particle with lifetime greater than 2 ns, for $0 < m_M < m_\pi$, from a similar analysis²⁴ are shown in Fig. 8.

Helicity suppression of $\pi \rightarrow e\nu$ would also be relaxed if a massive neutrino were emitted. Although the LEP experiments⁵ measuring the Z^0 width have demonstrated

that there are only three light conventional neutrinos, some extensions of the SM such as ones incorporating left-handed neutrino singlets ($\nu_{\chi_1}, \nu_{\chi_2}, \dots, \nu_{\chi_n}$)²⁸ lead to neutrino mixing without affecting the Z^0 width. If massive neutrinos exist and mixing occurs, weak eigenstates ν_{χ_l} may be related to mass eigenstates ν_l by a unitary matrix as in the case of quark mixing. Then, $\nu_l = \sum_{\chi=1}^{3+n} U_{l\chi} \nu_{\chi}$, where $l = e, \mu, \tau, \chi_1, \chi_2, \dots, \chi_n$. Such mixings would produce additional peaks in the positron energy spectrum from two body meson decays such as $\pi \rightarrow e\nu$.²⁷ The sensitivity to $|U_{ei}|^2$ increases as the helicity suppression effect relaxes with the increase of m_{ν_l} , but tends to decrease above $m_{\nu_l} \sim 80$ MeV due to the diminishing phase space.

The background suppressed $\pi \rightarrow e\nu$ spectrum in the latest TRIUMF experiment (Fig. 3b) was examined for evidence of peaks attributable to the presence of mass eigenstates ν_l .²⁹ The search was carried out by including in the fitting function an additional peak whose shape was derived from the shape-function obtained from the $\pi \rightarrow e\nu$ peak at 69 MeV stepped in 0.4 MeV increments through the energy range 8 to 61 MeV to find the most probable peak area at each energy. The distribution of the sample peak areas was consistent with random statistical fluctuations about a mean value of zero. The resulting upper limits for branching ratios normalized to the decay $\pi \rightarrow e\nu$ as a function of m_{ν_l} are shown by the solid curve in Fig. 9a. Upper limits on the mixing coefficients $|U_{ei}|^2$ for heavy neutrinos coupling to electrons were derived, and are plotted by the heavy solid curve A in Fig. 9b.

Another potential effect of massive neutrinos due to a relaxation of the helicity suppression would be to increase the $\pi \rightarrow e\nu$ branching ratio. Therefore, a deviation of $R_{\pi\tau}^{e\nu}$ from the value calculated assuming no neutrino mixing can also be used to constrain $|U_{ei}|^2$. Upper limits for $|U_{ei}|^2$ were calculated for $m_{\nu_l} < 55$ MeV as shown by the heavy dashed curve B in Fig. 9b.

5. Conclusion

Fig. 10 shows the history of measurements of the $\pi \rightarrow e\nu$ branching ratio. The recent experimental results have reduced the measurement uncertainties by a factor of three and are in excellent agreement with the SM prediction. Thus, the hypothesis of lepton universality is confirmed with greater precision and the generation puzzle persists. Future $\pi \rightarrow e\nu$ experiments may be able to reduce the experimental errors to the level of the theoretical uncertainties, further tightening the test of the SM. The best approach may be to fully exploit the timing distributions of $\pi - e$ and $\pi - \mu - e$ decays to reduce the sources of systematic uncertainties associated with the energy measurements. Theoretical developments to better determine the higher order terms in the lepton mass expansion of the radiative effects may also be feasible.

Although the structure dependent contribution to $\pi \rightarrow e\nu\gamma$ is small ($O(10^{-4})$ of $\pi \rightarrow e\nu$) its measurement represents an interesting opportunity for the study of low energy QCD effects.³³ It has been suggested that this process could reveal the presence of a small hypothetical tensor interaction.³⁴ $K \rightarrow e\nu\gamma$ decays where the structure dependent component is in the neighborhood of 50% may be more accessible for this purpose.

In the near future, calculable higher order processes may join the list of precise SM tests as rare K decay measurements become more sensitive. These are fertile testing grounds for the SM because the entire supposed particle spectrum of quarks, leptons, and gauge bosons can conceivably appear in internal loops. For the decay $K^+ \rightarrow \pi^+ \nu\bar{\nu}$ it has been demonstrated that, because the final state involves neutrinos rather than charged leptons, long distance effects are negligible compared with

short distance (i.e. fermion and gauge boson scale) internal processes.³⁵ $K^+ \rightarrow \pi^+ \nu \bar{\nu}$ is expected to occur at the level 1 to 3×10^{-10} in the SM where the uncertainty arises primarily from interesting undetermined parameters, the top quark mass and couplings, particularly, V_{td} . Thus, although it presents significant experimental challenges, $K^+ \rightarrow \pi^+ \nu \bar{\nu}$ may be the only higher order weak process which is both measurable with current facilities and is also subject to precise prediction. An experiment aimed at observing $K^+ \rightarrow \pi^+ \nu \bar{\nu}$, if it occurs within the SM range, is under way at Brookhaven National Laboratory.³⁶ In the longer term era of the proposed factories, B meson decays and other rare K decays such as $K_L^0 \rightarrow \pi^0 \nu \bar{\nu}$ which have distinct CP violation observables may join reactions like $\pi \rightarrow e \nu$ in providing precise standard model benchmarks free of strong interaction ambiguities.

6. Acknowledgement

I would like to thank W.J. Marciano for suggesting this article and for helpful comments and Toshio Numao for reading a draft of the manuscript.

References

1. See W.J. Marciano, *Ann. Rev. Nucl. and Particle Sci.*, (1992), to be published.
2. M. Shin and D. Silverman, *Phys. Lett.* **B213**, 379 (1988); S. Rajpoot and M. Samuël, *Mod. Phys. Lett.* **A3**, 1625 (1988). See also E. Ma, S. Pakvasa and S.F. Tuan, *Particle World* **3**, 27 (1992).
3. V. Barger, W.Y. Keung and S. Pakvasa, *Phys. Rev.* **D25**, 907 (1982).
4. O. Shanker, *Nucl. Phys.* **B204**, 375 (1982); see also J.F. Donoghue and L.F. Li, *Phys. Rev.* **D19**, 945 (1979); B. Williams and L.F. Li, *Nucl. Phys.* **B179**, 62 (1981); H.E. Haber, G.L. Kane and T. Stirling, *Nucl. Phys.* **B161**, 493 (1979).
5. See F. Dydak, *Proc. 25th Intern. Conf. on High Energy Physics*, Eds. K.K. Phua and Y. Yamazachi (S.E. Asia Theor. Phys. Assoc., and Phys. Soc. Japan, 1991) and ALEPH, DELPHI, L3 and OPAL Collaborations, CERN-PPE/91-232 (to be published).
6. S.M. Berman, *Phys. Rev. Lett.* **1**, 468 (1958).
7. T. Kinoshita, *Phys. Rev. Lett.* **2**, 477 (1959).
8. T. Goldman and W.J. Wilson, *Phys. Rev.* **D15**, 709 (1977).
9. W.J. Marciano and A. Sirlin, *Phys. Rev. Lett.* **36**, 1425 (1976).
10. W.J. Marciano, private communications.
11. D.A. Bryman *et al.*, *Phys. Rev.* **D33**, 1211 (1986).
12. D.I. Britton *et al.*, *Phys. Rev. Lett.* **68**, 3000 (1992).
13. E. DiCapua *et al.*, *Phys. Rev.* **133** (1964) B1333.
14. C. Zapek *et al.*, Bern University preprint LHEP-Preprint BUHE-92-1.
15. D.A. Bryman, *Phys. Rev.* **D46**, 1064 (1992).
16. W.J. Marciano and A. Sirlin, *Phys. Rev. Lett.* **61**, 1815 (1988).
17. *Rev. of particle properties*, K. Hikasa *et al.*, *Phys. Rev.* **D45**, S1 (1992).
18. J.Z. Bai *et al.*, *Phys. Rev. Lett.* **69**, 3021 (1992).
19. See W.J. Marciano, *Phys. Rev.* **D45**, R721 (1992) for a discussion and references.
20. J. Allaby *et al.*, *Phys. Lett.* **B179**, 301 (1986).
21. C. Albajar *et al.*, *Phys. Rev. Lett.* **B 185**, 233 (1987).
22. F. Abe *et al.*, (CDF Collaboration) *Phys. Rev. Lett.* **68**, 3398 (1992); F. Abe *et al.*, (CDF Collaboration) *Phys. Rev. Lett.* **69**, 28 (1992).
23. J. Alitti *et al.*, *Z. Phys.* **C52**, 209 (1991).
24. C.E. Picciotto *et al.*, *Phys. Rev.* **D37**, 1131 (1988).
25. R. Eichler *et al.*, *Phys. Lett.* **B 175**, 101 (1986).

26. G.B. Gelmini and M. Roncadelli, *Phys. Lett.* **99B**, 411 (1981).
27. R.E. Shrock, *Phys. Rev.* **D24** (1981) 1232; see also J.N. Ng, *Nucl. Phys.* **B191** 125, (1981).
28. L.S. Littenberg and R.E. Shrock, *Phys. Rev. Lett.* **68**, 443 (1992).
29. D.I. Britton *et al.*, *Phys. Rev.* **D46**, R885 (1992).
30. N. De Leener-Rosier, *et al.*, *Phys. Lett.* **B177**, 228 (1986).
31. G. Azuelos, *et al.*, *Phys. Rev. Lett.* **56**, 2241 (1986).
32. H.L. Anderson *et al.*, *Phys. Rev.* **119**, 2050 (1960).
33. See D.A. Bryman, P. Depommier and C. LeRoy, *Phys. Reports* **88**, 151 (1982).
34. V.N. Bolotov *et al.*, *Phys. Lett.* **B243** (1990) 308; A.A. Poblaguev, *Phys. Lett.* **B238**, 108 (1990).
35. D. Rein and L.M. Seghal, *Phys. Rev.* **D39**, 3325 (1989).
36. M.S. Atiya *et al.*, *Phys. Rev. Lett.* **64**, 21 (1990).

Table I TRIUMF $\pi \rightarrow e\nu$ branching ratio summary.¹²

Raw branching ratio $R(10^{-4})$	$1.1994 \pm 0.0034(\text{stat}) \pm 0.0023(\text{syst})$
Multiplicative corrections:	
Tail correction	1.0193 ± 0.0025
Pion stop time t_0	0.9998 ± 0.0008
Time calibration	1.0000 ± 0.0003
Monte Carlo	1.0027 ± 0.0011
V1 veto	1.0009 ± 0.0005
WC inefficiency	0.9998 ± 0.0004
π lifetime	1.0000 ± 0.0009
Branching ratio $R_{\text{exp}}^{\pi \rightarrow e\nu}(10^{-4})$	$1.2265 \pm 0.0034(\text{stat}) \pm (0.0044)(\text{syst})$

Table II PSI $\pi \rightarrow e\nu$ branching ratio corrections¹⁴

Process	Correction %	Error %
Electromagnetic losses	1.64	0.09
Photonuclear reactions	0.95	0.20
$\pi \rightarrow e\nu\gamma$ events with $E_{\text{total}} > 101$ MeV	0.04	0.02
Uncertainty of the energy calibration	0.0	0.08
$\pi \rightarrow e\nu$ self veto in anticounter	0.03	0.02
Time measurement difference for e and μ	-0.08	0.03
Pulse shape difference for e and μ	0.0	0.03
Efficiency of e^+ detection in target	0.15	0.01
Subtraction of radiative μ decay background	-1.13	0.17
Subtraction of pion reaction background	-0.45	0.02
Branching ratio $R_{\text{exp}}^{\pi \rightarrow e\nu}(10^{-4})$	1.235 ± 0.005	

Table III Values of g_e/g_μ .

Method	g_e/g_μ	Reference
$\sigma_{\mu}(\text{cc})/\sigma_{\nu}(\text{cc})$	1.10 ± 0.05	20
$\Gamma(W \rightarrow e\nu)/\Gamma(W \rightarrow \mu\nu)$	0.95 ± 0.10	21
$\Gamma(W \rightarrow e\nu)/\Gamma(W \rightarrow \mu\nu)$	0.99 ± 0.04	22
$\Gamma(\tau \rightarrow e\nu\nu)/\Gamma(\tau \rightarrow \mu\nu\nu)$	0.996 ± 0.010	
$\Gamma(\pi \rightarrow e\nu)/\Gamma(\pi \rightarrow \mu\nu)$	0.9985 ± 0.0015	
Average	0.9983 ± 0.0015	

Table IV Values of g_τ/g_μ .

Method	g_τ/g_μ	Ref.
$\Gamma(\tau \rightarrow e\nu\nu)/\Gamma(\mu \rightarrow e\nu\nu)$	0.980 ± 0.012	
$\Gamma(W \rightarrow \tau\nu)/\Gamma(W \rightarrow \mu\nu)$	0.96 ± 0.07	22
$\Gamma(\tau \rightarrow \pi\nu)/\Gamma(\pi \rightarrow \mu\nu)$	1.012 ± 0.021	
Average	0.987 ± 0.010	

Table V Values of g_τ/g_e .

Method	g_τ/g_e	Reference
$\Gamma(W \rightarrow \tau\nu)/\Gamma(W \rightarrow e\nu)$	$1.01 \pm 0.09 \pm 0.05$	21
$\Gamma(W \rightarrow \tau\nu)/\Gamma(W \rightarrow e\nu)$	$0.997 \pm 0.056 \pm 0.042$	23
$\Gamma(W \rightarrow \tau\nu)/\Gamma(W \rightarrow e\nu)$	0.97 ± 0.07	22
$\Gamma(\tau \rightarrow \mu\nu\bar{\nu})/\Gamma(\mu \rightarrow e\nu\bar{\nu})$	0.984 ± 0.012	
$\Gamma(\tau \rightarrow \pi\nu)/\Gamma(\pi \rightarrow e\nu)$	1.014 ± 0.021	
Average	0.991 ± 0.010	

Figure captions

1. (a) Feynman diagrams for Inner Bremsstrahlung in $\pi \rightarrow l\nu_l$ decay; (b) corrections for the $\pi \rightarrow l\nu_l$ decay due to virtual emission and reabsorption of photons; (c) diagrams which contribute in m_l terms (see Ref. 9).
2. Schematic view of the latest TRIUMF $\pi \rightarrow e\nu$ experimental setup.¹²
3. Positron energy spectrum (a) for early π decay times (< 30 ns), and (b) after background suppression.¹²
4. Time spectra for the upper ($\pi \rightarrow e\nu$) and lower ($\pi \rightarrow \mu - e$) parts of the energy spectrum.¹²
5. Setup for the PSI $\pi \rightarrow e\nu$ experiment. The last beam defining scintillator S, the active target T and the BGO calorimeter are shown.¹⁴
6. The total energy spectrum from the PSI experiment after cuts were applied. Three regions used to determine the branching ratio are indicated.¹⁴
7. The contribution to $\pi^+ \rightarrow e^+\nu_e$ of (a) charged Higgs bosons, (b) pseudoscalar leptoquarks, (c) vector leptoquarks and (d) supersymmetric particles.⁴
8. Branching ratio limits for $\Gamma(\pi \rightarrow e\nu M)/\Gamma(\pi \rightarrow \mu\nu)$ vs m_M .²⁴
9. Upper limits (90% C.L.) of (a) the branching ratio $\frac{\Gamma(\pi \rightarrow e\nu)}{\Gamma(\pi \rightarrow \mu\nu)}$ and (b) $|U_{e1}|^2$ for the neutrino mass up to 130 MeV. The results from Ref. 29 (curve A) and from Ref. 12 (curve B) are shown by the heavy lines. The previous limits by Azuelos *et al.*³¹ are shown by the thin solid curve C, and of De Leener-Rosier *et al.*³⁰ by the dashed curve D.
10. Measurements of the $\pi \rightarrow e\nu$ branching ratio. The standard model prediction is indicated.

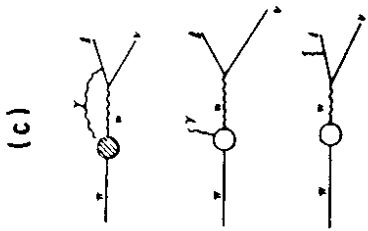
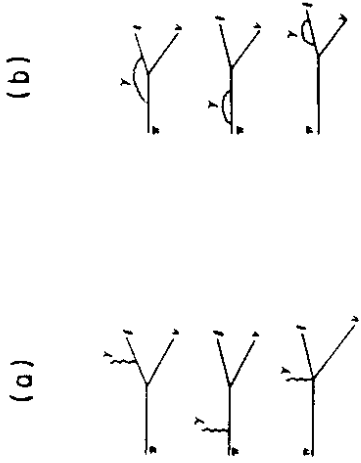


Fig. 1

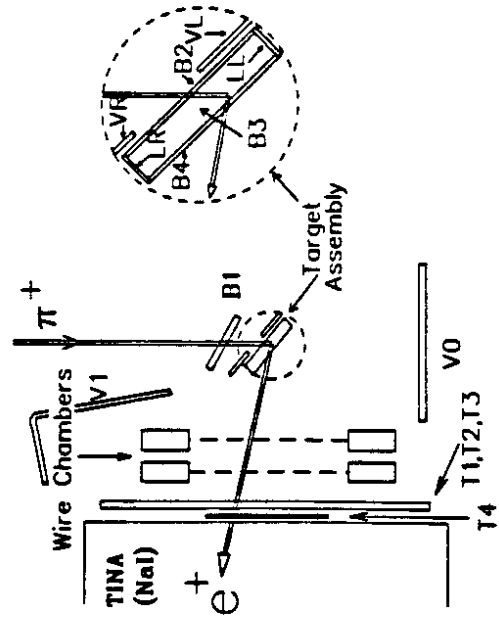


Fig. 2

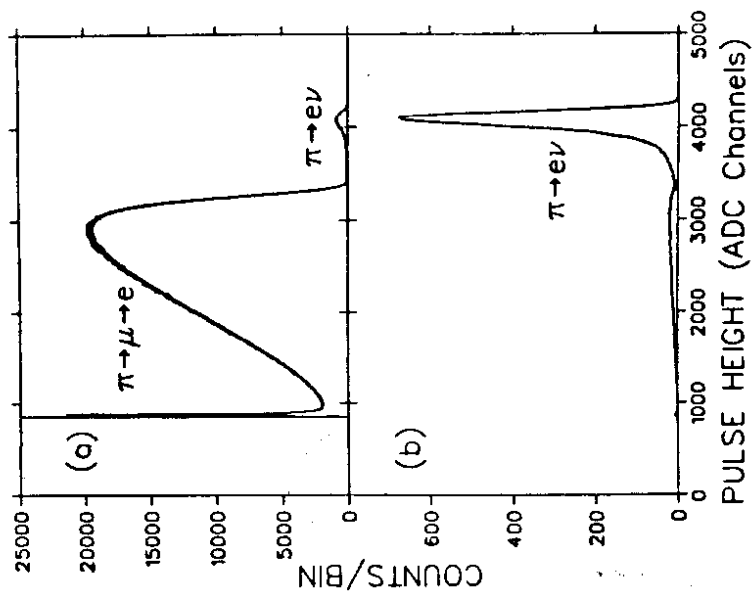


Fig. 3

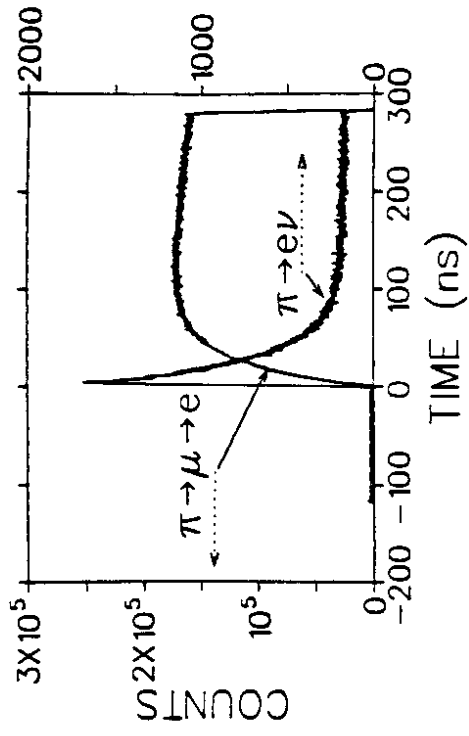


Fig. 4

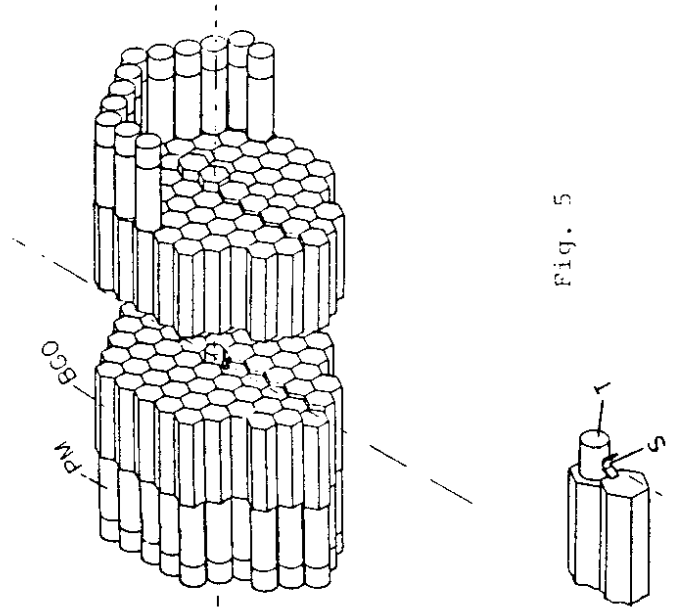


Fig. 5

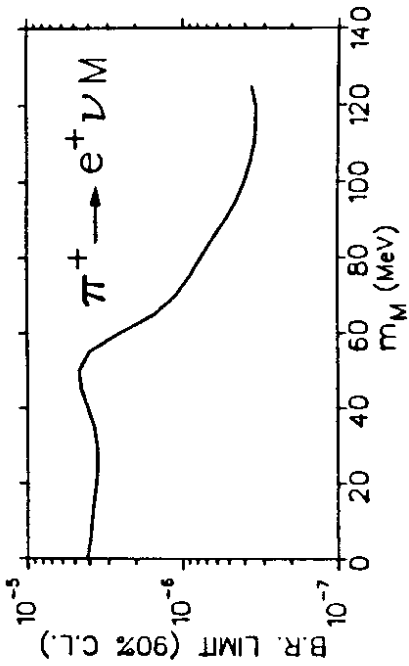


Fig. 8

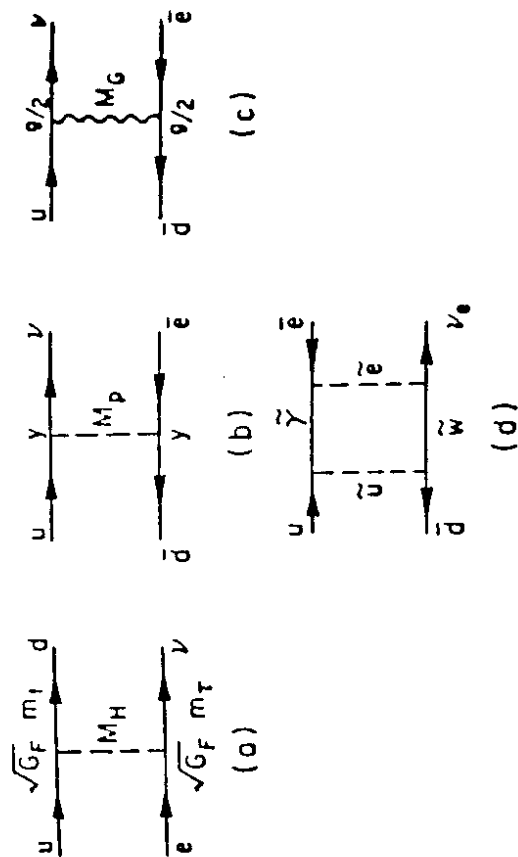
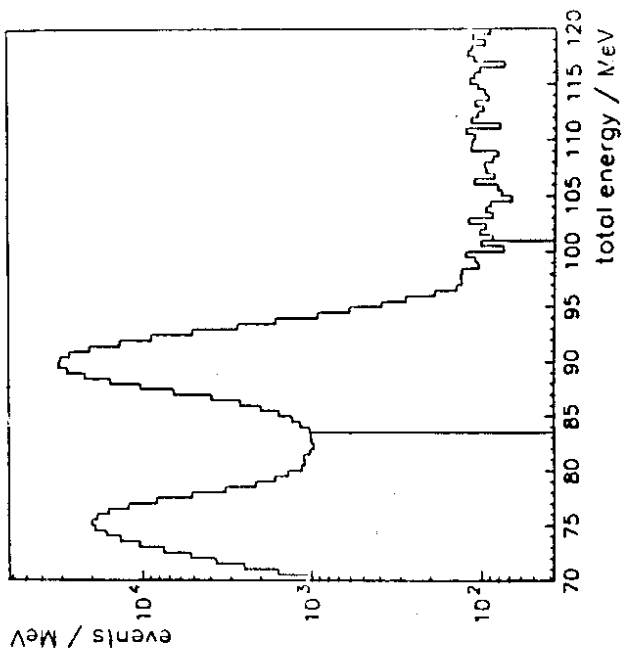


Fig. 6

Fig. 7

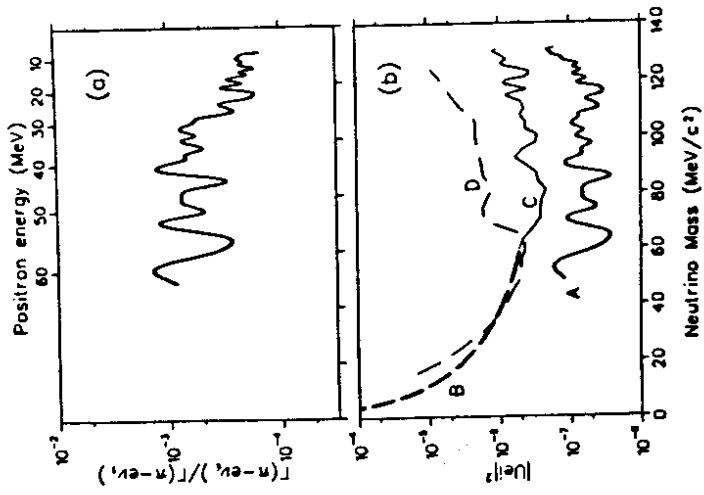


Fig. 9

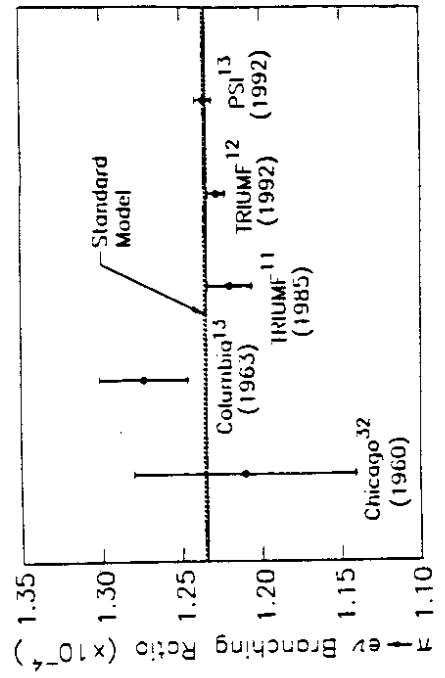


Fig. 10